

## Thermal Decomposition of Sodium Phosphates

Marcin Banach\* and Agnieszka Makara

Institute of Inorganic Chemistry and Technology, Cracow University of Technology, 24 Warszawska St., 31-155 Cracow, Poland

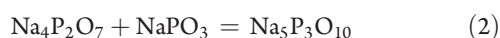
**ABSTRACT:** Sodium tripolyphosphate (STPP, Na<sub>5</sub>P<sub>3</sub>O<sub>10</sub>) was prepared by the thermal intermolecular dehydration of a spray-dried mixture of sodium phosphates, so that Na/P was 1.67. Thermal analysis, X-ray diffraction, Fourier transform infrared (FT-IR) analysis, and microscopic analysis with the application of a scanning electron microscope and an optical microscope with a heating system were applied in investigations. Temperatures of the formation of Na<sub>2</sub>H<sub>2</sub>P<sub>2</sub>O<sub>7</sub> (~463 K) and Na<sub>4</sub>P<sub>2</sub>O<sub>7</sub> (~488 K), as well as Na<sub>3</sub>P<sub>3</sub>O<sub>9</sub> (>513 K) and NaPO<sub>3</sub> (~593 K), were established for the process in which sodium tripolyphosphate is obtained. At over 616 K NaPO<sub>3</sub> melts and is the source of the liquid phase in the reaction system. The formation of anhydrous tripolyphosphate attains the highest speed around 563 K.

### INTRODUCTION

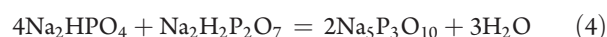
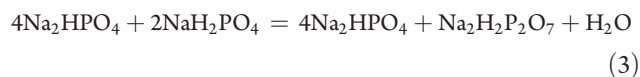
Sodium tripolyphosphate (STPP) is one of the most important condensed sodium phosphates because of its excellent detergent effects when it is used as an auxiliary washing agent (buffering properties, Ca<sup>2+</sup> and Mg<sup>2+</sup> ion sequestration, dirt particle deflocculation, and dispersion).<sup>1–3</sup> STPP is also used in the food industry for peptidization, sequestration, cross-linking of starch, and pH adjustment.<sup>4</sup>

STPP is mainly obtained in the process of the two-stage thermal dehydration of mixtures of sodium phosphates with a Na/P molar ratio of 1.67. Anhydrous STPP appears in two crystalline phases—phase 1 and phase 2. Phase 1 is formed at temperatures exceeding (723 to 773) K and phase 2 in temperatures reaching about 673 K. Both phase 1 and 2 are crystallized in a monoclinic system. The coordination of sodium ions is the main difference regarding their structure.<sup>5,6</sup>

The thermal dehydration of a mixture of sodium phosphate has been the subject of numerous investigations. Initially it was assumed that the molecular dehydration of the sodium orthophosphate mixture involves the formation of tetrasodium pyrophosphate and sodium metaphosphate, which later provide STPP.<sup>7</sup>

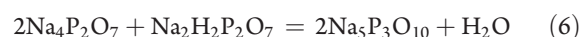
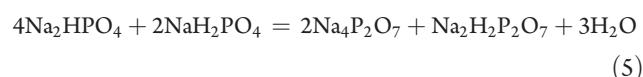


Results of the research carried out by Herr and Simon demonstrated that the reaction of STPP formation involves the intermediate formation of a mixture composed of disodium hydrogen orthophosphate and sodium dihydrogen pyrophosphate:<sup>8</sup>

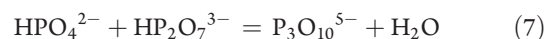


However, further studies led to the observation that the process involves the formation of a mixture of crystalline tetrasodium pyrophosphate and an amorphous phase of an elementary composition conforming with disodium dihydrogen pyrophosphate, containing

orthophosphates, metaphosphates, and higher pyrophosphates (tetra-, penta-).<sup>9</sup>



McGilvery and Scott, and later Edwards and Herzog, demonstrated that the basic reaction in which STPP is formed occurs on the interphase surface of the crystal-amorphous phase.<sup>9,10</sup>



Water released in the reaction hydrolyzes polyphosphates contained in the amorphous phase and therefore contributes to the formation of orthophosphates involved in the formation of tripolyphosphates.

The carried out studies show that the formation of STPP is associated with the occurrence of the liquid phase. The research was focused on the identification of phase transformations and the source of the liquid phase in the process for obtaining STPP.

These data are significant for the industrial production of sodium phosphate. Establishing the temperatures of sodium pyrophosphate, metaphosphate, and tripolyphosphate formation and the mechanism of phase transition will allow regulation of crystal phase content in the product and so its quality improvement. Additionally, it will be possible to determine the optimal parameters of the production process and will contribute to the cost decrease of sodium phosphate production, particularly STPPs.

### EXPERIMENTAL SECTION

The starting material of this work was a mixture of sodium phosphates obtained as a result of sodium phosphate solution spray drying in an STPP industrial installation. The solution of sodium phosphates was obtained by the neutralization of thermal phosphoric acid (in thermal methods for the production of

**Received:** February 15, 2011

**Accepted:** May 28, 2011

**Published:** June 08, 2011

phosphoric acid phosphorus is burned to obtain phosphoric anhydride, which is then hydrated) with sodium carbonate. The  $\text{Na}_2\text{O}:\text{P}_2\text{O}_5$  (TM) molar ratio for the neutralization process was 1.67.

An SDT 2960 simultaneous DTA-DTG TA thermoanalyzer was used to conduct thermal analysis of sodium phosphates. The measurements were performed in an air atmosphere within temperature ranges from (293 to 1073) K.

The instrument used in the investigations allows to carry out thermogravimetric (TG), differential thermogravimetric (DTG), and differential thermal (DTA) analyses simultaneously.

Thermogravimetry is based on recording of mass changes of a sample of material while heating or cooling, as a function of time or temperature, or on recording of mass changes of a material heated isothermally as a function of time.

As a result of thermogravimetric analysis a diagram (TG curve) was obtained, on which degrees reflecting sample mass loss during heating were marked. The degrees are diffused, and when there are more reactions taking place in the sample in sequence, they partly overlap. To improve readability of the TG curves a DTG analysis was conducted. This method gives the first derivative of thermogravimetric curve with respect to time. The

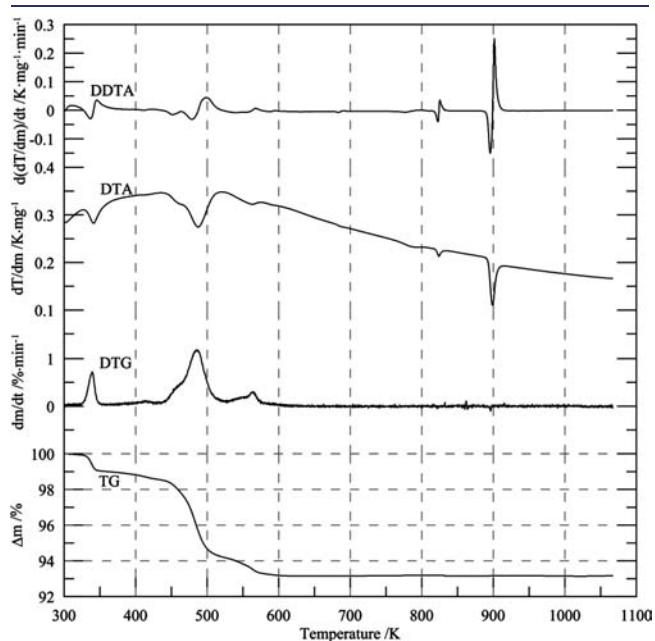


Figure 1. Results of thermal analysis of sodium phosphates.

DTG curve represents the rate of substance decomposition as a function of temperature. The complete loss of sample mass equals the peak area on this curve.

DTA stands for recording of temperature differences between the analyzed and the reference ( $\alpha\text{-Al}_2\text{O}_3$ ) substances with respect to time or temperature. It regards two samples which undergo identical treatment of heating or cooling in controllable environment. As a result of the measurement a DTA curve is obtained.

There are segments called baseline which can be found on the DTA curve. They denote temperature intervals in which no processes of heat absorption or release occur. During reaction or phase transition the baseline turns into peak. An endothermic peak occurs when the temperature of the analyzed sample is lower than of the reference sample. Conversely, the exothermic peak occurs when the temperature of the analyzed sample is higher than the reference one.

The DDTA curve is the first derivative of the DTA curve and is determined with the use of a graphical method. It represents the change in reaction speed with respect to temperature. Maximum values on this curve denote moments in which the speed of temperature decreases as a result of the reaction progress or its increased speed is maximum.

Infrared absorbance measurements were made of KBr pellets ( $w = 0.07$ ) over the range (400 to 1400)  $\text{cm}^{-1}$  using a Nicolet 5700 FTIR spectrometer with a high temperature analytical cell (Harric). All measurements were at 4  $\text{cm}^{-1}$  resolution.

An X-ray method with the use of a powder diffractometer D5005 (Bruker/AXS) with a high temperature reaction chamber XRK-900 (Anton Paar) was applied to identify the phase content of the investigated material. Cu K $\alpha$  radiation was used.

Photographs of grains were taken with a Nikon Eclipse LV100 optical microscope with a high temperature heating system TS1500 (Linkam). The samples were also identified by using a JEOL (JSM5510LV) scanning electron microscope.

A heating rate of 10  $\text{K}\cdot\text{min}^{-1}$  was used during X-ray, Fourier transform infrared (FT-IR), TA, and microscopic analysis.

## RESULTS

Figure 1 presents the results of the thermal analysis of spray-dried sodium phosphates, which allows for determining phase transformations occurring during the process of obtaining STPP.

Changes in the phase composition of the studied material during the process of STPP synthesis were identified based on the results of in situ X-ray analysis. Table 1 presents pooled data obtained for sodium phosphates calcinated directly in the high-temperature chamber of an X-ray apparatus.

Table 1. In Situ X-ray Analysis of Reaction Mixture

T/K	composition of the mixture at various stages of reaction						
as-prepared	$\text{Na}_2\text{HPO}_4 \cdot 2\text{H}_2\text{O}$	$\text{Na}_2\text{HPO}_4$	$\text{NaH}_2\text{PO}_4$	$\text{Na}_3\text{H}_3(\text{PO}_4)_2$	$\text{Na}_3\text{HP}_2\text{O}_7 \cdot \text{H}_2\text{O}$	$\text{Na}_4\text{P}_2\text{O}_7$	
343	$\text{Na}_2\text{HPO}_4 \cdot 2\text{H}_2\text{O}$	$\text{Na}_2\text{HPO}_4$	$\text{NaH}_2\text{PO}_4$	$\text{Na}_3\text{H}_3(\text{PO}_4)_2$	$\text{Na}_3\text{HP}_2\text{O}_7 \cdot \text{H}_2\text{O}$	$\text{Na}_4\text{P}_2\text{O}_7$	
413		$\text{Na}_2\text{HPO}_4$	$\text{NaH}_2\text{PO}_4$	$\text{Na}_3\text{H}_3(\text{PO}_4)_2$	$\text{Na}_3\text{HP}_2\text{O}_7 \cdot \text{H}_2\text{O}$	$\text{Na}_4\text{P}_2\text{O}_7$	
463				$\text{Na}_3\text{H}_3(\text{PO}_4)_2$		$\text{Na}_4\text{P}_2\text{O}_7$	$\text{Na}_2\text{H}_2\text{P}_2\text{O}_7$
488						$\text{Na}_4\text{P}_2\text{O}_7$	$\text{Na}_2\text{H}_2\text{P}_2\text{O}_7$
563						$\text{Na}_4\text{P}_2\text{O}_7$	$\text{Na}_3\text{P}_3\text{O}_9$ $\text{Na}_5\text{P}_3\text{O}_{10}$ (II)
593						$\text{Na}_4\text{P}_2\text{O}_7$	$\text{Na}_3\text{P}_3\text{O}_9$ $\text{Na}_5\text{P}_3\text{O}_{10}$ (II)
683						$\text{Na}_4\text{P}_2\text{O}_7$	$\text{Na}_5\text{P}_3\text{O}_{10}$ (II)
788						$\text{Na}_4\text{P}_2\text{O}_7$	$\text{Na}_5\text{P}_3\text{O}_{10}$ (II) $\text{Na}_5\text{P}_3\text{O}_{10}$ (I)
813						$\text{Na}_4\text{P}_2\text{O}_7$	$\text{Na}_5\text{P}_3\text{O}_{10}$ (I)
828						$\text{Na}_4\text{P}_2\text{O}_7$	$\text{Na}_5\text{P}_3\text{O}_{10}$ (I)

FT-IR spectra of the sodium phosphate sample obtained with using a high temperature analytical cell are shown in Figure 2. Their assignments are grouped in Table 2.

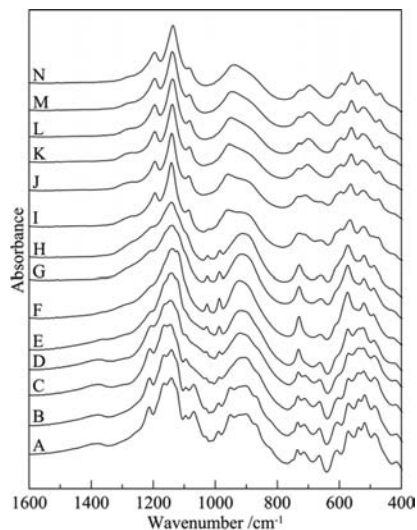


**Figure 2.** FT-IR spectra of sodium phosphate heated at various temperatures in a high temperature analytical cell: A, as-prepared; B, heated at (323 to 331) K; C, (375 to 385) K; D, (443 to 453) K; E, (468 to 478) K; F, (513 to 521) K; G, (573 to 581) K; H, (605 to 613) K; I, (663 to 670) K; J, (703 to 710) K; K, (763 to 770) K; L, (795 to 802) K; M, (813 to 820) K; N, (843 to 850) K.

X-ray diffraction analysis of the mixture of sodium phosphate showed that it consists of monosodium and disodium orthophosphate double salt ( $\text{NaH}_2\text{PO}_4 \cdot \text{Na}_2\text{HPO}_4$ ), disodium orthophosphate ( $\text{Na}_2\text{HPO}_4$ ), disodium orthophosphate dihydrate ( $\text{Na}_2\text{HPO}_4 \cdot 2\text{H}_2\text{O}$ ), sodium pyrophosphate ( $\text{Na}_4\text{P}_2\text{O}_7$ ), monosodium orthophosphate ( $\text{NaH}_2\text{PO}_4$ ), and trisodium pyrophosphate hydrate ( $\text{Na}_3\text{HP}_2\text{O}_7 \cdot \text{H}_2\text{O}$ ).

Adsorbed water is returned at a temperature about 348 K, and  $\text{Na}_2\text{HPO}_4 \cdot 2\text{H}_2\text{O}$  is degraded. These processes lead to a 1 % sample mass change due to water loss, which can be recorded on the TG curve. On the DTG curve these processes are represented as the endothermic effect with the extremum point at about 348 K. Bands visible in FT-IR spectra at (1068, 952, 825, and 752)  $\text{cm}^{-1}$  were assigned to asymmetric and symmetric stretching vibrations of the  $\text{PO}_3$  group and vibrations of the P–O–H group. They are characteristic for dihydrated disodium orthophosphate. The bands disappear when the temperature increases from (323 to 385) K, which confirms the dehydration of  $\text{Na}_2\text{HPO}_4 \cdot 2\text{H}_2\text{O}$ . The disappearance of disodium orthophosphate dihydrate salt was confirmed by the X-ray method (Table 1).

Within the temperature range from (453 to 473) K monosodium orthophosphate transformed into disodium dihydrogen pyrophosphate ( $\text{Na}_2\text{H}_2\text{P}_2\text{O}_7$ ). At these temperatures (1014 and 867)  $\text{cm}^{-1}$  bands characteristic of  $\text{NaH}_2\text{PO}_4$  disappear.  $\text{Na}_4\text{P}_2\text{O}_7$  is formed at temperatures from (473 to 523) K. The  $\text{Na}_2\text{H}_2\text{P}_2\text{O}_7$  and  $\text{Na}_4\text{P}_2\text{O}_7$  presence is confirmed by the X-ray method. A product formed altogether with  $\text{Na}_2\text{H}_2\text{P}_2\text{O}_7$  and  $\text{Na}_4\text{P}_2\text{O}_7$  is water, which is then removed from the system. As a result, a 4.5 % sample mass loss is to be found on the TG curve. The thermal

**Table 2.** FT-IR Spectra of Sodium Phosphate<sup>11–13</sup>

assignments	T/K														
	as-prepared	323 to 321	375 to 385	443 to 453	468 to 478	513 to 521	573 to 581	605 to 613	663 to 670	703 to 710	763 to 770	795 to 802	813 to 820	843 to 850	
	Wave Number/ $\text{cm}^{-1}$														
$\nu\text{P-O-H}$	1370	1370	1370	1370	1370	1370									
$\nu_{\text{as}}\text{P-O}_2$					1275	1275	1275	1275	1275	1275	1275	1275	1275	1275	
$\nu_{\text{as}}\text{P-O}_3$	1211	1211	1211	1211	1211	1211	1211	1211	1195	1195	1195	1195	1195	1195	
$\nu_{\text{as}}\text{P-O}_2$	1165	1165	1165	1165	1165	1165									
$\nu_{\text{s}}\text{P-O}_3, \nu_{\text{s}}\text{P-O}_2$	1141	1141	1141	1141	1141	1140	1140	1138	1138	1138	1138	1138	1138	1138	
$\nu_{\text{as}}\text{P-O}_2$	1122	1122	1122	1122	1122	1122	1122								
$\nu_{\text{as}}\text{P-O}_3$	1095	1095	1095	1095	1095	1095	1095	1095	1083	1083	1083	1083	1083	1083	
$\nu_{\text{as}}\text{P-O}_3$	1068	1068													
$\nu_{\text{as}}\text{P-O-P}$	1029	1029	1029	1029	1029	1029	1029	1029	1029						
$\nu_{\text{s}}\text{P-O}_3$	1014	1014	1014	1014											
$\nu_{\text{s}}\text{P-O}_3$	991	991	991	991	991	991	991	991							
$\nu_{\text{s}}\text{P-O}_3$	952	952							952	952	952	952	947	947	
$\nu_{\text{as}}\text{P-O}_3$	921	921	921	921	921	921	921	921	921						
$\nu_{\text{as}}\text{P-O-P}$	902	902	902	902	902	902	902	902	902	902	902	902	902	902	
$\nu\text{P-(O-H)}_2$	867	867	867	867											
$\nu\text{P-O-H}$	825	825													
$\nu\text{P-O-H}$	752	752													
$\nu_{\text{s}}\text{P-O-P}$	736	736	736	736	736	734	734	734	734	734	734	734	734	734	
$\nu_{\text{s}}\text{P-O-P}$	713	713	713	713					700	700	700	700	700	700	
$\delta(\text{O-P-O})$ and/or $\delta(\text{P=O})$	663	663	663	663	663	663	650	650	650	650					
	605	605	605	605	605	605	605	605	610	610	610	610	610	610	
									594	594	594	594	594	594	
	570	570	570	570	570	570	570	570	570	560	560	560	560	560	
	536	536	536	536	536										
	516	516	516	516	516	516	516	516	524	524	524	524	524	524	
	486	486	486	486	486	486	486	486	486	486					
	474	474	474	474	474				470	470	470	470	470	470	
	416	416	416	416	416	416	416	416	416	416	416	416	416	416	

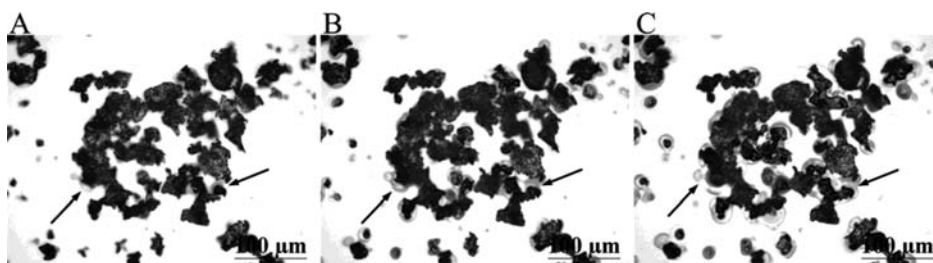


Figure 3. Microscopic photographs of sodium phosphate grains during calcination: A, 753 K; B, 793 K; C, 813 K.

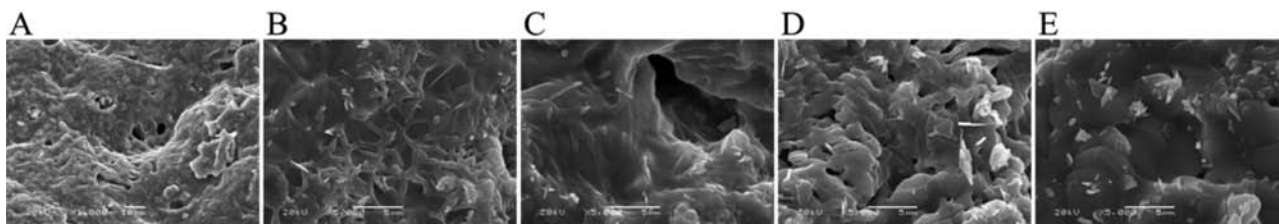


Figure 4. SEM microphotographs of STPP obtained at: A, 623 K; B, 673 K; C, 723 K; D, 773 K; E, 823 K.

effects are shown on the DTA curve as partly overlapping endothermic peaks with extremes at about (453 and 493) K.

At about 473 K phase 1 of anhydrous  $\text{Na}_5\text{P}_3\text{O}_{10}$  begins to form. The speed of its formation increases with further heating and reaches the maximum value at about 563 K. At this temperature the peaks on DTG curve representing change of speed reaction with respect to temperature and, on the DDTA curve which shows the speed of temperature change as a result of the reaction progress, reach their extremes. The process of  $\text{Na}_5\text{P}_3\text{O}_{10}$  forming is accompanied with about 1 % mass loss due to constitutional water removal (Figure 1).

In the FT-IR spectrum the last peaks assigned to orthophosphates [(1370, 1165, and 1122)  $\text{cm}^{-1}$ ] disappear when a temperature of 523 K is reached. However, the deformation of  $\text{PO}_2$  and  $\text{PO}_3$  groups associated with the formation of tetrasodium pyrophosphate, and then STPP becomes visible. Above this temperature the band assigned to sodium dihydrogen orthophosphate (1370  $\text{cm}^{-1}$ ) is also absent. At temperatures up to 723 K the structure of the condensate attains the form of phase 2. The transformation of phase 2 into phase 1 occurs within the range from (723 to 823) K. It is confirmed by X-ray analysis results presented in Table 1.

At temperatures from (573 to 663) K the FT-IR spectrum shows the structure of pyrophosphate, tripolyphosphate, and metaphosphates. Bands corresponding with metaphosphates are observed at (1270, 1195, 1138, 1095, 1029, 734, and 650)  $\text{cm}^{-1}$ . At temperatures from (613 to 663) K  $\text{Na}_3\text{P}_3\text{O}_9$  transforms into  $\text{NaPO}_3$ , which in the FT-IR spectrum is reflected by the disappearance of the 1029  $\text{cm}^{-1}$  band and the occurrence of (952, 700, 594, and 470)  $\text{cm}^{-1}$  bands.

At a temperature of about 683 K tetrasodium pyrophosphate becomes inverted, and it transforms from form V into form IV. Inversion to form III is visible on the DTA curve at temperatures close to 793 K.<sup>14</sup>

At about 823 K the melting of the eutectic between  $\text{NaPO}_3$  and  $\text{Na}_5\text{P}_3\text{O}_{10}$  is indicated by a break which is evident on the DTA curve. The thermal effect at 893 K is a peritectic point of the system  $\text{Na}_5\text{P}_3\text{O}_{10}\text{-Na}_4\text{P}_2\text{O}_7$ .<sup>15</sup>

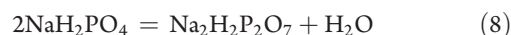
Figure 3 presents microscopic photographs of sodium phosphate grains during heating within the temperature range from (298 to 923) K. The use of an optical microscope equipped with a heating system enabled the observation of changes in the texture of the heated sample and the direct identification of the liquid phase presence during the calcination of sodium phosphates.

Significant amounts of the liquid phase were identified in microscopic images at a temperature of about 773 K. However, grain motions observed during the analysis at temperatures about 623 K may have resulted from the presence of low amounts of liquid on their surface.

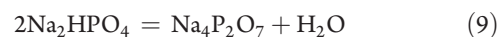
Figure 4 shows scanning electron microscopy (SEM) microphotographs of STPP obtained at temperatures from (623 to 823) K. The microstructure of STPP obtained at calcination temperatures from (623 to 673) K is characterized by the presence of oblong grains of the primary phase and fibrous grains of the solidified liquid phase. Such a system is formed when the liquid phase accounts only for an insignificant fraction of the material volume. The structure of STPP obtained at (723, 773, and 823) K is characterized by the presence of monocrystalline grains of the primary phase with well-formed flat sides interlinked by the solidified liquid phase.

## DISCUSSION

Heating of the mixture of sodium phosphates ( $\text{Na}_2\text{HPO}_4 \cdot 2\text{H}_2\text{O}$ ,  $\text{Na}_2\text{HPO}_4$ ,  $\text{NaH}_2\text{PO}_4$ ,  $\text{Na}_3\text{H}_3(\text{PO}_4)_2$ ,  $\text{Na}_3\text{HP}_2\text{O}_7 \cdot \text{H}_2\text{O}$ ,  $\text{Na}_4\text{P}_2\text{O}_7$ ) obtained during the spray drying of sodium orthophosphate solution up to a temperature about 463 K leads to the condensation of sodium dihydrogen orthophosphate to sodium dihydrogen pyrophosphate:



Combined water is discharged during this reaction. Further heating of the mixture up to 488 K results in the condensation of disodium hydrogen orthophosphate:





Tetrasodium pyrophosphate is the reaction product. Combined water is also discharged from the reaction system.

Further heating results in the formation of a crystalline mixture of  $\text{Na}_4\text{P}_2\text{O}_7$  and  $\text{Na}_3\text{P}_3\text{O}_9$ . Sodium trimetaphosphate is formed as the result of  $\text{Na}_2\text{H}_2\text{P}_2\text{O}_7$  melting over 513 K:<sup>16</sup>



At temperatures of about 593 K sodium trimetaphosphate decomposes to  $(\text{NaPO}_3)_x$ , which at temperatures over 616 K is in equilibrium with the liquid phase.<sup>17</sup> The liquid phase, as with the combined water, is produced in condensation reactions and facilitates diffusion of sodium and phosphate ions and therefore the crystallization of STPP.

The formation of anhydrous STPP begins as early as at 473 K and attains the highest speed close to 563 K. The process is described by eqs 2 and 6.

It was observed, similar to studies by Edwards and Herzog, that phase 1 STPP is formed in the range of lower temperatures (about 488 K).<sup>10</sup> Further heating at first results in the transformation of phase 1 into phase 2, and then phase 1 is again formed at higher temperatures from (723 to 773) K.

Van Wazer explained the occurrence of the high-temperature phase 1 within the lower temperature range (phase 2 range of stability), transformation of phase 1 into phase 2, and after reaching the phase 1 stability temperature the back transformation of phase 2 into phase 1 by the Gay-Lussac–Ostwald principle, known as the step rule.<sup>17</sup> According to this rule, if several phases of reaction exist, the thermodynamically unstable phase is formed as the first one, transforming later to the stable phase.

## CONCLUSION

The carried out studies show that the formation of sodium tripolyphosphate is associated with the occurrence of the liquid phase. The research was focused on the identification of phasic transformations and the source of the liquid phase in the process for obtaining STPP. It was established, based on thermal analysis, X-ray in situ analysis, in situ FT-IR, and microscopic analysis that during the heating of a mixture of phosphoric salts present in a spray-dried mixture of sodium phosphates at temperatures from (453 to 493) K sodium dihydrogen orthophosphate converts to disodium dihydrogen pyrophosphate and disodium hydrogen orthophosphate to tetrasodium pyrophosphate. The formation of STPP attains the highest speed at about 563 K.

Sodium dihydrogen pyrophosphate exposed to temperatures over 513 K produces sodium trimetaphosphate, which decomposes to sodium metaphosphate at about 593 K. At over 616 K  $\text{NaPO}_3$  melts and is the source of the liquid phase in the reaction system.

The transformation of a low-temperature phase STPP into a high-temperature phase occurs at temperatures from (723 to 773) K. The temperature of 823 K corresponding to the highest yield of phase 1 STPP is the temperature of eutectic point for the  $\text{Na}_5\text{P}_3\text{O}_{10}$ – $\text{NaPO}_3$  system.

## AUTHOR INFORMATION

### Corresponding Author

\*Tel.: +4812 628 28 61. Fax: +4812 628 20 36. E-mail: marcinbanach@chemia.pk.edu.pl.

## REFERENCES

- (1) Arai, H.; Maruta, I.; Kariyone, T. Study of Detergency. II. Effect of Sodium Tripolyphosphate. *J. Am. Oil Chem. Soc.* **1965**, *43*, 315–316.
- (2) Köhler, J. Detergent Phosphates: an EU Policy Assessment. *J. Bus. Chem.* **2006**, *3*, 15–30.
- (3) Yangxin, Y.; Jin, Z.; Bayly, A. E. Development of Surfactants and Builders In Detergent Formulations. *Chin. J. Chem. Eng.* **2008**, *16*, 517–527.
- (4) Hourant, P. General Properties of the Alkaline Phosphates: Major Food and Technical Applications. *Phosphorus Res. Bull.* **2004**, *15*, 85–94.
- (5) Corbridge, D. E. C. The Crystal Structure of Sodium Triphosphate,  $\text{Na}_5\text{P}_3\text{O}_{10}$ , Phase I. *Acta Crystallogr.* **1960**, *13*, 263–269.
- (6) Davies, D. R.; Corbridge, D. E. C. The Crystal Structure of Sodium Triphosphate,  $\text{Na}_5\text{P}_3\text{O}_{10}$ , Phase II. *Acta Crystallogr.* **1958**, *11*, 315–319.
- (7) Dombrowski, H. M. About Reaction of Triphosphate Formation while Mono- and Disodium Phosphate are Thermally Dehydrated. *Russ. J. Inorg. Chem.* **1962**, *7*, 95.
- (8) Herr, W.; Meyer-Simon, E. A Contribution to the Reaction of Tripolyphosphate Formation. *J. Chem. Sci.* **1951**, *6B*, 462–463.
- (9) McGilvery, J. D.; Scott, A. E. The Role of Water in the Formation of Sodium Triphosphate by Calcination. *Can. J. Chem.* **1954**, *32*, 1100–1111.
- (10) Edwards, J. W.; Herzog, A. H. The Mechanism of Formation of Sodium Triphosphate from Orthophosphate Mixtures. *J. Am. Chem. Soc.* **1957**, *79*, 3647–3650.
- (11) Chapman, A. C.; Thirlwell, L. E. Spectra of Phosphorus Compounds-I, The Infrared Spectra of Orthophosphates. *Spectrochim. Acta* **1964**, *20*, 937–947.
- (12) Moustafa, Y. M.; El-Egili, K. Infrared Spectra of Sodium Phosphates Glasses. *J. Non-Cryst. Solids* **1998**, *240*, 144–153.
- (13) He, Z.; Heneycutt, W.; Xing, B.; McDowell, R. W.; Pellechia, P. J.; Zhang, T. Solid-State Fourier Transform Infrared and <sup>31</sup>P Nuclear Magnetic Resonance Spectral Features of Phosphate Compounds. *Soil Sci.* **2007**, *172*, 501–515.
- (14) Partridge, E. P.; Hicks, V.; Smith, G. W. A Thermal Microscopic and X-Ray Study of the System  $\text{NaPO}_3$ – $\text{Na}_4\text{P}_2\text{O}_7$ . *J. Am. Chem. Soc.* **1941**, *63*, 454–466.
- (15) Quimby, O. T. The Chemistry of Sodium Phosphates. *Chem. Rev.* **1947**, *40*, 141–179.
- (16) Thilo, E. The Structural Chemistry of Condensed Inorganic Phosphates. *Angew. Chem.* **1965**, *23*, 1056–1066.
- (17) Van Wazer, J. R. *Phosphorus and Its Compounds*; Interscience Publishers Inc.: New York, 1958.